

Water-Enabled Visual Detection of DNA

Yonghui Liu, Huaxin Yao, and Jin Zhu*

Department of Polymer Science and Engineering, School of Chemistry and Chemical Engineering, State Key Laboratory of Coordination Chemistry, Nanjing National Laboratory of Microstructures, Nanjing University, Nanjing 210093, China

S Supporting Information

ABSTRACT: A water-enabled visual detection strategy has been developed for the sequence-specific identification of target DNA. The conceptual basis of the assay scheme, water condensation, is environmentally friendly and chemical transformation-free, thus offering significant assay advantages over conventional diagnostic systems. This label-free strategy operates on a target-driven generation of a hydrophilic structure and alteration of surface wettability and, consequently, transition of morphological state of and light propagation mode in the surface-condensed water. The chip array detection system, implemented herein with the ligase chain reaction-rolling circle amplification protocol, has allowed the achievement of high sensitivity (600 copies), high selectivity (single-base discrimination specificity), and multiplexed analysis capability.

Innovation in chemistry has been constantly driven by the need for a fundamental understanding of molecular basis for life. Herein, the call for an environmentally friendly DNA detection system has enabled the elaboration of a surface chemistry that allows the control of morphological state of and light propagation mode in the surface-condensed water. We have recently developed a variety of chemical and biological tools for DNA molecular diagnostics.¹ Through these efforts, we envisioned that a label-free, chip-based array architecture with direct spotting fabrication and parallel visualization/imaging capabilities would offer significant assay advantages. We report herein a water-enabled visual detection (WEVD) strategy for the on-chip identification of target DNA (Figure 1). Briefly, a target-triggered generation of a hydrophilic structure and alteration of surface wettability (from lower affinity to higher affinity for water) leads to a transition of the morphological state (from discrete droplet to uniform thin film) of and light propagation mode (from diffuse reflection/light scattering to light transmission) in the surface-condensed water.² With the use of a typical chip substrate, silicon, the transmission of the light will give a pristine, darkened outlook of the surface on the target-containing spot, and diffuse reflection/light scattering will render the target-free spot a bright appearance. Unlike conventional schemes (e.g., label-based, enzyme-linked immunosorbent assay³), the signal amplification step in our WEVD strategy, water condensation, is inherently a label-free process devoid of any chemical transformation as it occurs whenever the chip temperature is below the dew point (dictated by the relative humidity, or RH). The readout of target can in principle be achieved with a diversity of wettability alteration approaches

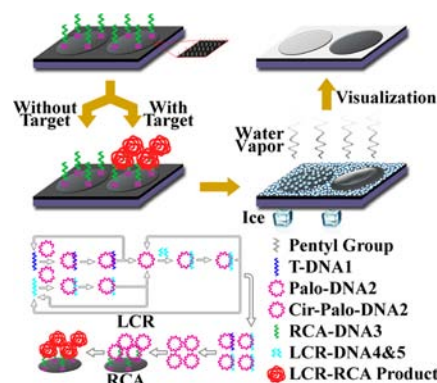


Figure 1. Schematic illustration of WEVD-based on-chip detection of DNA. A silicon chip spotted with RCA-DNA3 is challenged with a sample containing or lacking target T-DNA1. A hydrophilic product is generated only when T-DNA1 is present, triggering the alteration of surface wettability for water (from lower affinity to higher affinity; note that the pentyl group is important for the achievement of a desired degree of initial surface hydrophobicity). This leads to a transition of the morphological state (from discrete droplet to uniform thin film) of and corresponding light propagation mode (from diffuse reflection/light scattering to light transmission) in the surface-condensed water. The transmission of light gives a darkened outlook on the target-containing spot, and diffuse reflection/light scattering gives a bright outlook on the target-free spot. The WEVD strategy is implemented herein with the LCR-RCA protocol (bottom left), with the assistance of Palo-DNA2 and LCR-DNA4/LCR-DNAs, intermediate LCR product Cir-Palo-DNA2, and final LCR-RCA product.

(e.g., target-enabled delivery of a hydrophilic structure) and chip materials (e.g., for a transparent glass slide, visualization against a darkened backdrop). The WEVD strategy, implemented herein with the ligase chain reaction (LCR)⁴-rolling circle amplification (RCA)⁵ protocol, has afforded an assay method with high sensitivity (600 copies of DNA target), high selectivity (single-base discrimination specificity), and multiplexed analysis capability in a direct spot array fabrication/visualization/imaging format.

Molecular diagnostics has been conventionally achieved in either the in-solution or on-chip format.⁶ The in-solution assay format offers homogeneous one-phase operation simplicity,⁷ but the benefit per se poses severe constraints on the types of readout signals that can be utilized (e.g., fluorescence) and the number of distinct targets that can be multiplexed (even for suspension arrays⁸). The diversification of readout signals is desired for the

Received: July 18, 2013

Published: October 21, 2013

achievement of scenario-dependent assay versatility,⁹ and multiplexed analysis is crucial for the comprehensive understanding of interwoven biological networks.¹⁰ The on-chip assay format differs fundamentally from the in-solution assay format by virtue of the involvement of both liquid and solid macroscopic phases.¹¹ The phase separation promises massively parallel storage of information and high-density multiplexed analysis of targets in an array architecture, through the assistance of a diversity of label-free (recording of a change in the device property effected by the target-binding perturbation of phase boundary, e.g., dielectric property)¹² and label-based (e.g., fluorescence) strategies.¹¹ However, the translation of a signal readout scheme into such an array architecture can sometimes be a daunting, if not impossible, task. Indeed, label-free strategies generally take advantage of the vertically thin phase boundary for the generation of a delicate signal, as such a further decrease in the signal level through the shrinking of lateral dimension on an array spot can be catastrophic and can result in susceptibility to nonspecific background or even erratic readout. More importantly, challenges frequently come from the miniaturized fabrication of each individual detection module and complicated adaptation of the assay architecture for the acquisition of array signal (e.g., imaging). Currently the array architecture has been primarily implemented with label-based, scanning-compatible strategies (especially fluorescence imaging). Albeit largely functional, these strategies suffer from complicated and labor-intensive synthetic chemistry and the use of environmentally harmful labels. The WEVD strategy reported herein provides a robust solution to the issues associated with the on-chip assay format through the adoption of an environmentally friendly, chemical transformation-free, and array architecture-compatible water condensation signal amplification process.

The feasibility of WEVD strategy for DNA detection was initially evaluated with a ligation-RCA protocol on a sequence associated with the anthrax lethal factor (T-DNA1, for information on all the DNA sequences, see Table S1).¹ This protocol requires the participation of two probe DNA strands: a padlock DNA (Palo-DNA2), and a primer DNA (RCA-DNA3, with a flexible A₁₀ spacer and a thiol anchor, amenable to surface immobilization). The sequences of Palo-DNA2 and RCA-DNA3 are designed such that T-DNA1 and RCA-DNA3 can recognize disparate portions of Palo-DNA2. As noted above, key to the implementation of WEVD strategy is a DNA chip with an appropriate hydrophobicity. The following surface modification procedure ensures the generation of such an assay-ready chip: coupling of hydroxyl group on a thoroughly cleaned silicon chip (specifically, on the surface of naturally formed silicon oxide layer) with 3-(2-aminoethylamino)propyltrimethoxysilane (EDAS); reaction of amino group with *N*-succinimidyl 4-(*N*-maleimidomethyl)cyclohexane-1-carboxylate (SMCC); passivation of unreacted amino group with hexanoic anhydride (HA); spotting of RCA-DNA3 for the covalent conjugation with maleimido group; passivation of unreacted maleimido group with 1-hexanethiol (HT) (a step that can be omitted without causing deleterious effect on the assay performance).

A typical assay experiment starts with the sealing of the nick junction of Palo-DNA2 (with *Taq* or T4 DNA ligase). A reaction at 45 °C for 4 h in the presence of T-DNA1 allows the efficient generation of circularized Palo-DNA2 (Cir-Palo-DNA2) (Figures S1, S2). The selection of 45 °C for the elimination of background reaction derives from the fact that T-DNA1/Palo-DNA2 duplex is close to the fully dehybridized state at this temperature (Figure S3). Cir-Palo-DNA2 can be purified

through an initial removal of the linear T-DNA1 (with exonucleases I and III) and a subsequent extraction with ZipTip (Figure S4). Both in-solution (extension of a nonthiolated primer DNA, RCA-DNA3E) (Figures S5, S6) and on-chip (extension of RCA-DNA3) (Figure S7) RCA reaction (with ϕ 29 DNA polymerase) can be effected on the Cir-Palo-DNA2 template. Importantly, the on-chip RCA reaction affords a covalently linked, long and tandem single-strand DNA. This long single-strand DNA product enables the required alteration of surface wettability. A defining characteristic of the WEVD strategy is the rapid generation of signal. Thus, incubation of a precooled chip (on ice) for merely 2 min in a 30 °C, 45 ± 5% RH atmosphere allows the spot signal to be directly visualized by the naked eye, or if permanent recording of the signal is preferred, imaged by a digital camera (originally grayscale image, convertible to color-scale image, Figures 2A and S8). A caveat

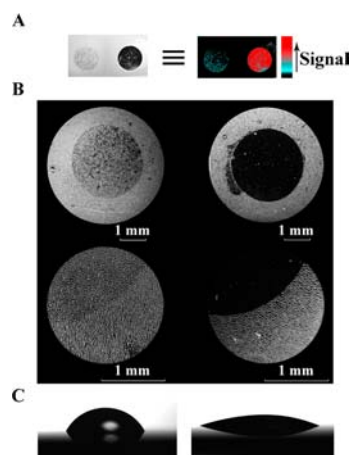


Figure 2. Implementation of WEVD-based on-chip DNA detection with the ligation-RCA protocol. (A) Macroscopic image (grayscale, left panel) of the spot in the absence (left) and presence (right) of 1 μ M T-DNA1. For image visualization/analysis, the original grayscale image can be converted into a color-scale image (right panel) using an industry standard GenePix Pro 6 microarray analysis software (Molecular Devices). The direction that the arrow is pointing represents the signal intensity increase direction. (B) Optical microscopic image of the spot in the absence (left) and presence (right) of 1 μ M T-DNA1 (top and bottom images for low- and high-magnification view). Discrete droplets have been observed in both the primer-derivatized, target-free area (26 μ m in diameter, 963/mm² in density) and the primer-free area (20 μ m, 1317/mm²),^{2a} and formation of uniform thin film is apparent in the primer-derivatized, target-containing area. (C) Macroscopic image of water droplet, for contact angle measurement, in the primer-derivatized area after ligation-RCA reaction in the absence (left) and presence (right) of 1 μ M T-DNA1.

to this environmentally friendly approach is that water condensation, a critical step for the reproducible generation of signal, should be stringently controlled. The key is the precise regulation of temperature (atmosphere and chip) and RH in a closed chamber and exact timing of condensation duration. In general, under otherwise identical condition, a higher RH translates to a faster onset of signal. Importantly, the chip can undergo repeated write (water condensation)/read (spot signal visualization)/erase (drying of surface with a compressed gas) operations without the deterioration of signal, thus ensuring the ultimate acquisition of authentic assay result. An alternative assay format is through the exhalation of moisture (37 °C, 100% RH) from a human being onto the chip surface (below 25 °C). A glass

slide can be used if placed against a black plastic backdrop (Figure S9).

Two experimental observations pertaining to the surface hydrophobicity deserve attention: (1) The coverage of alkyl group with a long enough chain length (pentyl group as generated in the case of passivation with HA) is critical for the achievement of a desired degree of hydrophobicity, as passivation with acetic anhydride (methyl group) affords a relatively inferior assay surface. (2) The hydrophobicity requirement also warrants a strict control of primer reaction condition (10 μM loading concentration, 37 $^{\circ}\text{C}$ /6 h in a humid environment); certain conditions (100 μM primer loading concentration, overnight reaction, or reaction in a dried atmosphere) can render the primer-derivatized area too hydrophilic to be useful. On an additional note, the HA passivation step should be carried out at $\sim 15^{\circ}\text{C}$ for the assurance of assay integrity. The above ligation-RCA protocol allows for the detection of target at 0.1 nM (10 μL) (Figure S8).

Direct evidence for the morphological state transition of surface-condensed water as the basis for signal generation has been obtained by optical microscopy observation (Figure 2B). As a consequence of the transition, discrete droplets capable of diffuse reflection/light scattering give a bright-looking target-free spot, whereas uniform thin film capable of light transmission furnishes a visually dark target-containing spot. This detection capability can be rationalized by the alteration of water contact angle (i.e., surface wettability) in the presence of target (Figures 2C and S10, Table S2). The critical threshold contact angle for water for the transition of its morphological state from discrete droplet to uniform thin film has been established to be $\sim 40^{\circ}$.^{2a,b} Indeed, the contact angle is $\sim 57^{\circ}$ for the primer-derivatized area (as compared to $\sim 64^{\circ}$ for the primer-free area); after the ligation-RCA step, this value remains virtually unchanged ($\sim 66^{\circ}$) for the target-free spot but is changed to $\sim 22^{\circ}$ for the target-containing spot.

Although the rudimentary working principle of WEVD-based DNA detection strategy has been unambiguously proven by the ligation-RCA protocol described above, the low sensitivity warrants further improvement. The cascade amplification version of the ligation step, LCR, is ideally suited for the seamless integration with the RCA reaction. For the LCR reaction to occur, two additional short DNA amplicons (blunt-end design; forward, LCR-DNA4, and reverse, LCR-DNA5) are required. A screening of the ligases indicates that *Taq* DNA ligase is best suited for the LCR-based amplification of *Palo-DNA2*. In addition, *Taq* DNA ligase is the enzyme of choice when single-base discrimination is demanded. The optimized LCR condition, 16 cycles of either (65 $^{\circ}\text{C}$, 30 s/25 $^{\circ}\text{C}$, 2 min/45 $^{\circ}\text{C}$, 3 min) (for sensitivity experiments, vide infra) or (65 $^{\circ}\text{C}$, 30 s/45 $^{\circ}\text{C}$, 5 min) (for single-base discrimination and multiplexed analysis experiments, vide infra), allows the amplified generation of LCR product, *Cir-Palo-DNA2*, exclusively in the presence of T-DNA1 (Figures S11–S15). The pinpoint accuracy offered by our blunt-end LCR obviates the need for a more intricate version of the LCR (e.g., single-base overhang LCR,^{13a} gap LCR^{13b}).

The optimized LCR condition allows one to examine the DNA detection sensitivity with the LCR-RCA protocol. The *Cir-Palo-DNA2* product generated with LCR (with single-strand DNA, T-DNA1, LCR-DNA4 and LCR-DNA5, and ligation product from LCR-DNA4 and LCR-DNA5, digested) can be either directly loaded into the RCA reaction mixture or undergo a prior ZipTip extraction process. The direct loading approach, as used throughout herein, avoids any uncertainty that might arise

from the recovery of *Cir-Palo-DNA2*, thus ensuring better reproducibility of the assay result. With this LCR-RCA protocol, one can visually observe a distinct signal at a target concentration as low as 0.1 fM, corresponding to a detection limit of 600 copies of DNA in 10 μL of sample. This detection limit can also be independently confirmed from the digitally recorded image (Figures S16 and 3), which permits either qualitative (by visual distinction) or quantitative (by averaging the pixel value in a specific channel) evaluation of signal intensity on each spot.

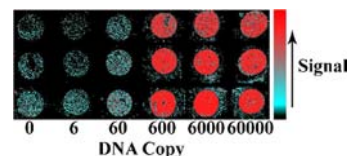


Figure 3. WEVD-based on-chip DNA detection with the LCR-RCA protocol. Macroscopic image of the spot in the presence of T-DNA1. From left to right (each column containing 3 spots for triplicate experiment): T-DNA1 (10 μL) concentration of 0 M, 1 aM, 10 aM, 0.1 fM, 1 fM, 10 fM.

Genetic variations are ubiquitous in nature and provide the basis for phenotypic trait diversity. The ability to discriminate between a fully complementary target and a sequence with a single-base mismatch site¹⁴ is important for many biomedical applications (e.g., screening for genetic diseases). Many assays use a thermal-stringency wash^{9b,15} (with an elevated temperature) to meet the demanding selectivity requirement. Here the high fidelity associated with the *Taq* DNA ligase endows isothermal single-base discrimination specificity at the ligation stage. Indeed, single-round ligation of *Palo-DNA2* at 45 $^{\circ}\text{C}$ for 4 h occurs exclusively in the presence of T-DNA1 (Figure S14). The sealing efficiency of the nick junction is negatively impacted by a mismatched base. In fact, no product can be observed for samples containing single-base mismatched sequences examined herein (SBM1 through SBM6), regardless of the location of the mismatch site: middle of forward amplicon (SBM1), nick site of forward amplicon (SBM2), one-base away from the nick site of reverse amplicon (SBM3), nick site of reverse amplicon (SBM4 and SBM5), middle of reverse amplicon (SBM6). Maintenance of the ligation specificity in the LCR amplification step (Figure S15) should offer assay selectivity advantages for the LCR-RCA protocol. Consistent with this conjecture, through such a protocol, single-base mismatches can be readily identified with the WEVD strategy (Figures S17 and 4), thus proving its superior strand distinguishing capability.

The WEVD strategy allows for an array configuration through a simple spotting procedure and the readout of signal in a highly parallel fashion. These two features make the strategy inherently

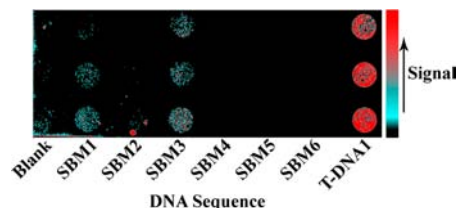


Figure 4. WEVD-based on-chip single-base discrimination with the LCR-RCA protocol. Macroscopic image of the spot in the presence of T-DNA1 (0.1 nM) or a single-base mismatched sequence (SBM1 through SBM6, 0.1 nM), or in the absence of any DNA (blank).

amenable to multiplexing, and with appropriate engineering tools, to miniaturization and automation. Multiplexed analysis is important for the acquirement of a systemic view of the breadth and diversity of biological entities.^{10,16} The multiplexing capability demonstrated herein employs a two-target (T-DNA1 and T-DNA6) sample as the test case. For the assay of the second target (T-DNA6), a distinct set of DNA strands, including padlock DNA (Palo-DNA7), surface primer (RCA-DNA8), and two LCR amplicons (forward, LCR-DNA9, and reverse, LCR-DNA10), needs to be designed. Of particular importance is the avoidance of cross-hybridization and cross-ligation between the DNA strands individually targeting T-DNA1 and T-DNA6 (Figures S18, S19). With the possibility of cross-interference eliminated, the two-target detection can indeed be achieved (Figures S20 and 5); a distinct signal can be observed for the corresponding primer-derivatized spot in, and only in the presence of each respective target.

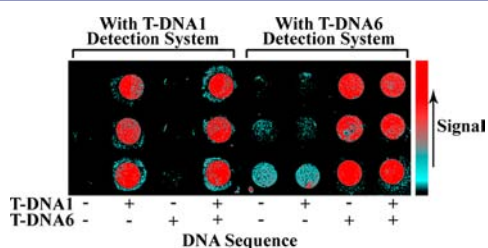


Figure 5. WEVD-based on-chip two-target detection with the LCR-RCA protocol. Macroscopic image of the spot in the presence of T-DNA1 (0.1 nM) and/or T-DNA6 (0.1 nM). The plus (+) and minus (-) signs at the bottom of each column indicate the presence and absence of a particular target, respectively.

In conclusion, a label-free, water-enabled on-chip DNA assay strategy has been reported. The assay relies on the transition of light propagation mode in morphologically distinct surface-condensed water for the signaling of target. The WEVD strategy has been implemented in a direct spot array readout format and features high sensitivity, high selectivity, and multiplexed analysis capability. Given recent advances in the tailored control of morphological state of surface-condensed water, the underlying detection principle documented herein is likely extendable to the assay of other types of biological targets.

■ ASSOCIATED CONTENT

Supporting Information

Materials and methods, DNA detection data. This material is available free of charge via the Internet at <http://pubs.acs.org>.

■ AUTHOR INFORMATION

Corresponding Author

jinz@nju.edu.cn

Notes

The authors declare no competing financial interest.

■ ACKNOWLEDGMENTS

J.Z. gratefully acknowledges support from the National Natural Science Foundation of China (21274058) and the National Basic Research Program of China (2013CB922101, 2011CB935801).

■ REFERENCES

- (1) (a) Shu, X.; Liu, Y.; Zhu, J. *Angew. Chem., Int. Ed.* **2012**, *51*, 11006. (b) Zhou, X.; Xia, S.; Lu, Z.; Tian, Y.; Yan, Y.; Zhu, J. *J. Am. Chem. Soc.* **2010**, *132*, 6932. (c) Zhou, X.; Cao, P.; Tian, Y.; Zhu, J. *J. Am. Chem. Soc.* **2010**, *132*, 4161. (d) Hong, M.; Zhou, X.; Lu, Z.; Zhu, J. *Angew. Chem., Int. Ed.* **2009**, *48*, 9503. (e) Qiu, F.; Jiang, D.; Ding, Y.; Zhu, J.; Huang, L. *Angew. Chem., Int. Ed.* **2008**, *47*, 5009.
- (2) (a) Briscoe, B. J.; Galvin, K. P. *Sol. Energy* **1991**, *46*, 191. (b) Grosu, G.; Andrzejewski, L.; Veilleux, G.; Ross, G. G. *J. Phys. D: Appl. Phys.* **2004**, *37*, 3350. (c) Howarter, J. A.; Youngblood, J. P. *Macromol. Rapid Commun.* **2008**, *29*, 455. (d) Howarter, J. A.; Youngblood, J. P. *Adv. Mater.* **2007**, *19*, 3838. (e) Liu, K.; Jiang, L. *Annu. Rev. Mater. Res.* **2012**, *42*, 231. (f) Liu, K.; Yao, X.; Jiang, L. *Chem. Soc. Rev.* **2010**, *39*, 3240. (g) Cebeci, F. C.; Wu, Z.; Zhai, L.; Cohen, R. E.; Rubner, M. F. *Langmuir* **2006**, *22*, 2856. (h) Nuraje, N.; Asmatulu, R.; Cohen, R. E.; Rubner, M. F. *Langmuir* **2011**, *27*, 782. (i) Park, K.-C.; Choi, H. J.; Chang, C.-H.; Cohen, R. E.; Mckinley, G. H.; Barbastathis, G. *ACS Nano* **2012**, *6*, 3789.
- (3) Lequin, R. M. *Clin. Chem.* **2005**, *51*, 2415.
- (4) (a) Barany, F. *Proc. Natl. Acad. Sci. U.S.A.* **1991**, *88*, 189. (b) Cao, W. *Trends Biotechnol.* **2004**, *22*, 38. (c) Wiedmann, M.; Wilson, W. J.; Czajka, J.; Luo, J.; Barany, F.; Batt, C. A. *Genome Res.* **1994**, *3*, S51–S64. (5) (a) Nilsson, M.; Malmgren, H.; Samiotaki, M.; Kwiatkowski, M.; Chowdhary, B. P.; Landegren, U. *Science* **1994**, *265*, 2085. (b) Fire, A.; Xu, S.-Q. *Proc. Natl. Acad. Sci. U.S.A.* **1995**, *92*, 4641. (c) Craw, P.; Balachandran, W. *Lab Chip* **2012**, *12*, 2469.
- (6) Debnath, M.; Prasad, G. B. K. S.; Bisen, P. S. *Molecular Diagnostics: Promises and Possibilities*; Springer: Dordrecht, 2010.
- (7) (a) Wang, K.; Tang, Z.; Yang, C. J.; Kim, Y.; Fang, X.; Li, W.; Wu, Y.; Medley, C. D.; Cao, Z.; Li, J.; Colon, P.; Lin, H.; Tan, W. *Angew. Chem., Int. Ed.* **2009**, *48*, 856. (b) Zhu, C.; Liu, L.; Yang, Q.; Lv, F.; Wang, S. *Chem. Rev.* **2012**, *112*, 4687. (c) Ho, H. A.; Najari, A.; Leclerc, M. *Acc. Chem. Res.* **2008**, *41*, 168. (d) Prusty, D. K.; Herrmann, A. *J. Am. Chem. Soc.* **2010**, *132*, 12197.
- (8) (a) Lin, C.; Jungmann, R.; Leifer, A. M.; Li, C.; Levner, D.; Church, G. M.; Shih, W. M.; Yin, P. *Nat. Chem.* **2012**, *4*, 832. (b) Nicewarner-Peña, S. R.; Freeman, R. G.; Reiss, B. D.; He, L.; Pena, D. J.; Walton, I. D.; Cromer, R.; Keating, C. D. *Science* **2001**, *294*, 137. (c) Pregibon, D. C.; Toner, M.; Doyle, P. S. *Science* **2007**, *315*, 1393. (d) Li, Y.; Cu, Y. T.; Luo, D. *Nat. Biotechnol.* **2005**, *23*, 885. (e) Han, M.; Gao, X.; Su, J. Z.; Nie, S. *Nat. Biotechnol.* **2001**, *19*, 631. (f) Lee, H.; Kim, J.; Kim, H.; Kim, J.; Kwon, S. *Nat. Mater.* **2010**, *9*, 745. (g) Braeckmans, K.; De Smedt, S. C.; Roelant, C.; Leblans, M.; Pauwels, R.; Demeester, J. *Nat. Mater.* **2003**, *2*, 169. (h) Fournier-Bidoz, S.; Jennings, T. L.; Klostranec, J. M.; Fung, W.; Rhee, A.; Li, D.; Chan, W. C. *Angew. Chem., Int. Ed.* **2008**, *47*, 5577.
- (9) (a) Giljohann, D. A.; Mirkin, C. A. *Nature* **2009**, *462*, 461. (b) Rosi, N. L.; Mirkin, C. A. *Chem. Rev.* **2005**, *105*, 1547.
- (10) Donnelly, P. *Nature* **2008**, *456*, 728.
- (11) Bilitewski, U. *Microchip Methods in Diagnostics*; Humana: New York, 2009.
- (12) (a) Ohno, Y.; Maehashi, K.; Matsumoto, K. *J. Am. Chem. Soc.* **2010**, *132*, 18012. (b) Brousseau, L. C., III. *J. Am. Chem. Soc.* **2006**, *128*, 11346. (c) Markov, D. A.; Swinney, K.; Bornhop, D. J. *J. Am. Chem. Soc.* **2004**, *126*, 16659. (d) Homola, J. *Chem. Rev.* **2008**, *108*, 462. (e) Fritz, J.; Baller, M. K.; Lang, H. P.; Rothuizen, H.; Vettiger, P.; Meyer, E.; Güntherodt, H.-J.; Gerber, C.; Gimzewski, J. K. *Science* **2000**, *288*, 316. (f) Zheng, G.; Patolsky, F.; Cui, Y.; Wang, W. U.; Lieber, C. M. *Nat. Biotechnol.* **2005**, *23*, 1294.
- (13) (a) Kälén, I.; Shephard, S.; Candrian, U. *Mutat. Res. Lett.* **1992**, *283*, 119. (b) Abravaya, K.; Carrino, J. J.; Muldoon, S.; Lee, H. H. *Nucleic Acids Res.* **1995**, *23*, 675.
- (14) (a) Sassolas, A.; Leca-Bouvier, B. D.; Blum, L. J. *Chem. Rev.* **2008**, *108*, 109. (b) Banoub, J. H.; Newton, R. P.; Esmans, E.; Ewing, D. F.; Mackenzie, G. *Chem. Rev.* **2005**, *105*, 1869.
- (15) Cutler, J. I.; Auyeung, E.; Mirkin, C. A. *J. Am. Chem. Soc.* **2012**, *134*, 1376.
- (16) (a) Hanash, S. M.; Pitteri, S. J.; Faca, V. M. *Nature* **2008**, *452*, 571. (b) Hood, L.; Heath, J. R.; Phelps, M. E.; Lin, B. *Science* **2004**, *306*, 640.